Dynamic transition in driven vortices across the peak effect in superconductors

Mahesh Chandran,* R. T. Scalettar, and G. T. Zimányi
Department of Physics, University of California, Davis, California 95616
(Received 8 October 2002; revised manuscript received 3 January 2003; published 27 February 2003)

We study the zero-temperature dynamic transition from the disordered flow to an ordered flow state in driven vortices in type-II superconductors. The transition current I_p is marked by a sharp kink in the $V(I)$ characteristic with a concomitant large increase in the defect concentration. On increasing magnetic field B, the $I_p(B)$ follows the behavior of the critical current $I_c(B)$. Specifically, in the peak effect regime $I_p(B)$ increases rapidly along with I_c. We also discuss the effect of varying disorder strength on I_p.

DOI: 10.1103/PhysRevB.67.052507 PACS number(s): 74.25.Qt, 74.25.Sv

The model of driven interacting particles in presence of quenched disorder captures essential features of the dynamics occurring in many condensed matter systems. Of specific interest is the dynamics of vortices above the critical (or depinning) current I_c in type II superconductors. Early numerical simulation of the transport characteristics in two dimensions (2D) showed that the topological defects are generated close to I_c, and are annealed at high driving force.[1] This suggested a dynamic transition from the disordered flow to an ordered flow at a current $I_p > I_c$. Theoretically, Koshelev and Vinokur (KV) considered this transition at I_p similar to an equilibrium "melting" transition of a clean system in the moving reference frame.[2] The effect of quenched disorder on the moving vortices is included in the theory through an effective shaking temperature $T_{\mathrm{sh}} \propto I^{-1}$. In Koshelev-Vinokur theory, the recrystallization current I_p increases as $(T_m - T)^{-1}$ on approaching the equilibrium melting temperature T_m of the static system. Later calculations[3–5] and simulations[6–9] identified the free flowing state above I_p as the smectic phase. In the smectic phase, the particles move in static channels with quasi-long-range order perpendicular to the flow compared with liquidlike short-range order within the channels.[10]

The dynamic transition in driven vortices was first studied experimentally in the transport measurements by Bhattacharya and Higgins (BH),[12] and was later observed in neutron scattering[11] and Bitter decoration[13] experiments. BH studied the behavior of transition current I_p as a function of the magnetic field B, particularly in the peak effect (PE) regime. The PE is marked by a rapid increase in $I_c(B)$, generally close to the upper critical field B_{c2}. BH found that the $I_p(B)$ increases rapidly in the field range in which the PE occurs. This behavior of $I_p(B)$ in the PE regime is similar to the behavior of $I_p(T)$ around T_m as observed in simulation by KV in Ref. 2. The similarity can be traced to the softening of the shear modulus c_{66} of the vortex lattice. But an important difference separates the two: unlike BH, KV do not see any corresponding increase in $I_c(T)$, i.e., no peak effect in the $I_c(T)$ is observed in the simulation. This makes it difficult to correlate the increase in $I_p(T)$ close to T_m to the enhanced coupling of the vortex lattice to the quenched disorder. The increase in $I_p(T)$ could very well be due to increased thermal fluctuations on approaching T_m, thus requiring larger currents to anneal the lattice defects.

Recently, we showed that the PE occurs in a system of 2D vortices close to B_{c2} at zero temperature.[14] In this paper, we revisit the dynamic transition, particularly across the PE. We find that $I_p(B)$ increases rapidly in the field range in which the $I_c(B)$ shows the PE. The dynamic transition at I_p is characterized by hysteresis in $V(I)$ and a sharp peak in the dynamic resistance $R_d(I)$. The topological defect concentration also shows a jump at I_p. We present the dynamic phase *I-B* diagram, and discuss the effect of increasing the disorder strength Δ on I_p.

Consider a 2D cross section of a bulk type-II superconductor perpendicular to the magnetic field $\mathbf{B} = B\hat{\mathbf{z}}$. Within London's approximation, the dynamics of vortices are governed by the overdamped equation of motion

$$\eta \frac{d\mathbf{r}_i}{dt} = -\sum_{j \neq i} \nabla U^v(\mathbf{r}_i - \mathbf{r}_j) - \sum_k \nabla U^p(\mathbf{r}_i - \mathbf{R}_k) + \mathbf{F}_{\mathrm{ext}}.$$

Here η is the flux-flow viscosity, and the first term represents the intervortex interaction given by the potential $U^v(r) = (\phi_0^2/8\pi^2\lambda^2)K_0(\tilde{r}/\lambda)$, where K_0 is the zeroth-order Bessel function and $\tilde{r} = (r^2 + 2\xi^2)^{1/2}$. λ and ξ are the penetration depth and coherence length of the superconductor, respectively. ϕ_0 represents the flux quantum. The vortex pinning is added through the second term which is an attractive interaction with parabolic potential wells $U^p(r) = U_0(r^2/r_p^2 - 1)$ for $r < r_p$, and 0 otherwise, centered at the random $\mathbf{R}_k$ locations. The third term $\mathbf{F}_{\mathrm{ext}} = (1/c)\mathbf{J} \times \phi_0\hat{\mathbf{z}}$ is the Lorentz force due to transport current density $\mathbf{J}$. The length is in units of $\lambda(B=0) = \lambda_0$, and J is in units of cf_0/ϕ_0 where $f_0 = \phi_0^2/8\pi^2\lambda_0^3$. The time t is in units of $\eta\lambda/f_0$ whereas the velocity v of vortices is in units of f_0/η.

We use the reduced magnetic field $b = B/B_{c2}$ with $B_{c2} = \phi_0/2\pi\xi^2$, and it is calculated from the lattice constant $a_0/\lambda = (4\pi/\sqrt{3})^{1/2}(1/\kappa^2 b)^{1/2}$. The B dependence of λ is $\lambda(b) = \lambda_0/(1-b^2)^{1/2}$, with a similar expression for ξ. The simulation is for the Ginzburg-Landau parameter $\kappa = \lambda/\xi = 10$ which is typical of the low-T_c materials. The number of vortices N_v was chosen in the range of 800–1200. The prefactor U_0 of the pinning potential is distributed randomly between $\Delta \pm 0.01$. The results presented below are for the pin density $n_p = 2.315$. We calculate the transport characteristics $V(I)$, where the current $I \propto J_y$, and the voltage $V \propto \langle v_x \rangle$. The topological defect concentration $f_d(I)$ is obtained by De-

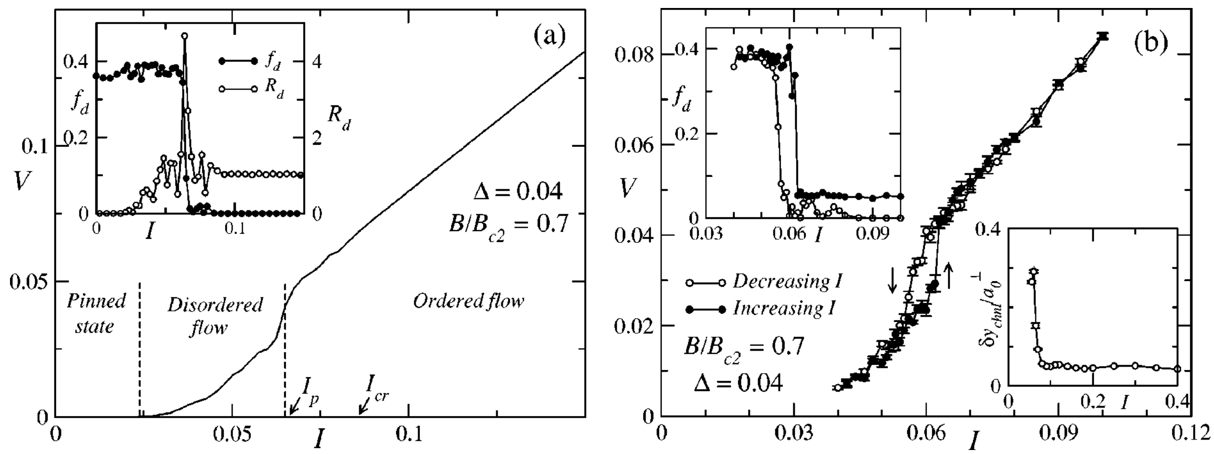

FIG. 1. (a) The $V(I)$ characteristics for $\Delta = 0.04$ and $b = 0.7$. Inset: the defect concentration $f_d(I)$ and the dynamic resistance $R_d(I)$. (b) Hysteresis in $V(I)$ and $f_d(I)$ (upper inset) across I_p. The lower inset shows $(\delta y_{\mathrm{chnl}})/a_0^{\perp}$, where $a_0^{\perp} = (\sqrt{3}/2)a_0$ and a_0 is the lattice constant.

launay triangulation of the real space configuration. We choose the free flowing vortex lattice at high driving currents as the initial configuration, and decrease the current to 0 in small steps across I_c. This particular method of preparing the system minimizes the influence of nonequilibrium defects which are present in field cooled simulations. The equation of motion is time integrated by standard techniques. The $V(I)$ and $f_d(I)$ are time averaged in the steady state. Parallel algorithms were employed to speed up the simulation at high densities.[15]

Figure 1(a) shows the $V(I)$ curve for $b = 0.7$ and $\Delta = 0.04$. Broadly, three current regimes can be identified: (a) a pinned state for $I < I_c$, (b) a disordered flow state between $I_c < I < I_p$ where some vortices remain immobile and large transverse excursions of the active channels are present, and (c) an ordered flow state for $I > I_p$ with all vortices moving and interchannel hopping takes place with, at most, neighboring channels. The $f_d(I)$, and the dynamic resistance $R_d(I) = dV/dI$ is plotted in the inset of Fig. 1(a). The current I_p is marked by a sharp peak in $R_d(I)$ and a large change in f_d. The response function $V(I)$ shows a kink at I_p, as evident from Fig. 1(a). We find that $V(I)$ and $f_d(I)$ are also hysteretic across I_p, as shown in Fig. 1(b). The kink and the hysteresis in the response function $V(I)$ suggests that the dynamic transition occurs at I_p. The transition is of first order nature, as was identified in Ref. 2.

In Fig. 2, real space configurations are shown for currents above and below I_p corresponding to parameters in Fig. 1. The instantaneous configuration shows a relatively ordered lattice above I_p. The vortex trajectories are well separated channels aligned parallel to v_x. The average transverse wandering of the channel $\langle \delta y_{\mathrm{chnl}} \rangle < \alpha a_0^{\perp}$, where $a_0^{\perp} = (\sqrt{3}/2)a_0$ and a_0 is the lattice constant and $\alpha \approx 0.05$. Just below I_p, α becomes ≈ 0.3, as shown in the inset of Fig. 1(b). The slowing down of vortices effectively couples the transverse velocity component v_y to the quenched disorder. This induces large scale dislocations, and the dynamic friction ($\propto R_d$) increases. The increase in transverse wandering of vortices is also reflected in the dense braiding of the active channels. The behavior of $\langle \delta y_{\mathrm{chnl}} \rangle$ across I_p is similar to the Lindemann criterion for thermal melting. Note that some of the vortices appear as immobile for $I = 0.555$ in Fig. 2(b) (right panel). The region of immobile vortices grow with decreasing I until I_c is reached when the whole system is pinned.

The $R_d(I)$ has been used previously to identify the phase boundary. In Ref. 12, the transition from the disordered flow to the ordered flow state is identified as the current at which $R_d(I) \approx R_{\mathrm{BS}}$ where R_{BS} is the asymptotic Bardeen-Stephen flux-flow resistance. This current is marked as I_{cr} in Fig. 1(a). In Ref. 8, the state between I_p and I_{cr} is identified as the smectic phase, whereas above I_{cr}, the state is defined as a transversely frozen phase. The later state is distinguished from the smectic phase by the absence of transverse jumps by vortices between adjacent channels.

We note that neither $V(I)$ nor $f_d(I)$ shows any feature at I_{cr}. Therefore, a more appropriate description of the state between I_p and I_{cr} is possible in terms of fluctuation which allows occasional transverse excursions of the vortices between adjacent channels. The rate of such transverse jumps can be calculated by employing Arrhenius relation which is

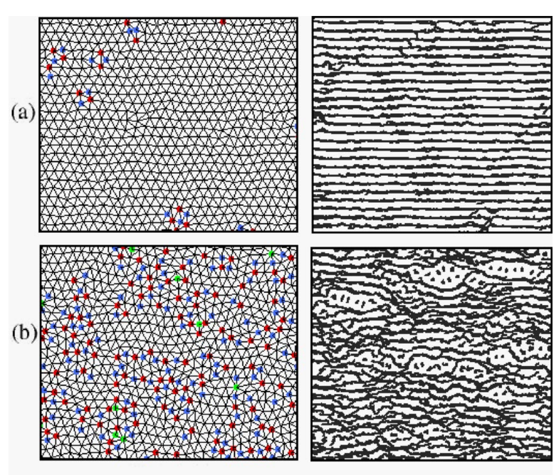

FIG. 2. Instantaneous vortex configuration (left) and vortex trajectories (right) for (a) $I = 0.06 > I_p$ and (b) $I = 0.055 < I_p$. The $b = 0.7$ and $\Delta = 0.04$.

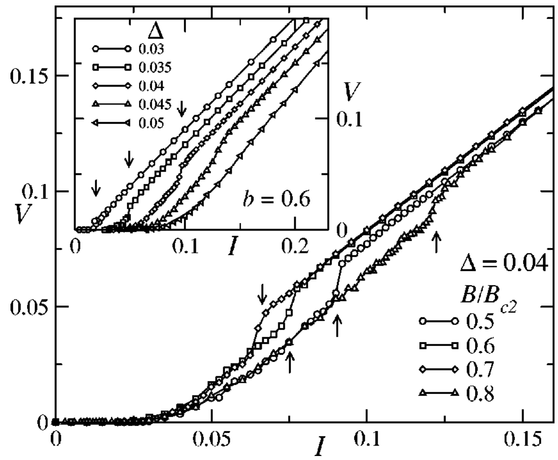

FIG. 3. $V(I)$ curves for $\Delta = 0.04$ for fields across the PE. Inset: $V(I)$ curves for increasing disorder strength Δ for $b=0.6$. The curves in the inset are shifted horizontally by 0.01. The arrows mark the transition current I_p.

conventionally used to describe thermal activation over energy barrier, but with temperature replaced by $T_{\rm sh}$.[16] Such a description can account for the suppression of transverse jumps above I_{cr}, and also for the experimentally observed $R_d(I)$ curves. To summarize, the dynamic transition in the moving lattice occurs at I_p at which the dynamic resistance $R_d(I)$ shows a peak. The flowing state above I_p is a smectic phase with small longitudinal correlation and quasi-long-range order in the transverse direction.

We now consider the behavior of I_p as the magnetic field $b = B/B_{c2}$ is changed, particularly across the PE in $I_c(b)$. For $\Delta = 0.04$, the onset field for PE is $b_{op} \approx 0.75$ whereas the peak occurs at $b_{\rm peak} \approx 0.9$. Figure 3 shows the $V(I)$ curves for four values of b between 0.5 and 0.8. The I_p can be easily identified by the sharp kink in the $V(I)$ curves. With increasing b, the I_p first decreases before increasing rapidly in the PE field regime. The $f_d(I)$ and $R_d(I)$ characteristics across I_p are similar to that shown in Fig. 1 for all values of b. In the inset of Fig. 3, the effect of increasing disorder strength Δ on I_p is shown for $b = 0.6$. Other than the expected increase in I_p with increasing Δ, we find that the transition at I_p is broadened for $\Delta \geqslant 0.05$. Also, the hysteresis in $V(I)$ across I_p is too small to be distinguished. This suggests that the first-order nature of the dynamic transition at I_p does not survive for $\Delta \geqslant 0.05$.

Figure 4(a) shows the dynamic phase diagram *I-B* for $\Delta = 0.04$ which summarizes the main result of the paper. The $I_p(b)$ and $I_c(b)$ shows similar behavior as b approaches the upper critical field value. Particularly, the rapid increase in $I_p(b)$ coincide with the peak effect in $I_c(b)$. The region between $I_p(b)$ and $I_c(b)$ constitutes the disordered flow regime, whereas above I_p vortices flow in ordered channels. For $\Delta = 0.04$, the $I_p(b) = k(b_0 - b)^{-1}$ with $b_0 = 0.92$ and $k = 0.015$ gives a reasonable fit for $b > b_{op}$, as shown by the thick line in Fig. 4(a). This form of $I_p(b)$ was motivated by the behavior of $I_p(T)$ on approaching the equilibrium melting transition in Ref. 2. The *I-B* plot in Fig. 4(a) thus supports the picture that both the static and the dynamic friction of the vortex system increases rapidly in the field range in which the peak effect occurs. As shown in Ref. 14, the PE in the critical current I_c is driven by the softening of the vortex interaction on approaching the upper critical field B_{c2}. Softening of the vortex interaction also reduces the shaking temperature $T_{\rm sh} \propto I^{-1}$ required for the dynamic ordering (or recrystallization) of the vortices which explains the increase in $I_p(b)$ in the PE regime. Thus, an increase in I_c (as a function of B or T) implies an increase in I_p. We emphasize that the reverse does not hold, i.e., increase in I_p *does not* imply an increase in I_c. This can be seen from the behavior of $I_p(T)$ and $I_c(T)$ in Ref. 2 where thermal depinning causes $I_c(T)$ to decrease monotonically even as $I_p(T)$ increases on approaching the equilibrium melting temperature T_m. Overall, we find the behavior of $I_p(B)$ and $I_c(B)$ in good agreement with the experimental observation.[12]

Figure 4(b) shows the I_c and the I_p as a function of Δ for $b = 0.6$. For the system size used in the simulation ($N_v \sim 1000$), the depinning transition is elastic for $\Delta \leqslant 0.03$ (hence, $I_p = I_c$), whereas for $\Delta \geqslant 0.05$, $I_p \propto \Delta$. The two disorder regimes can be identified as the weak pinning and the strong pinning regime, respectively. The crossover from

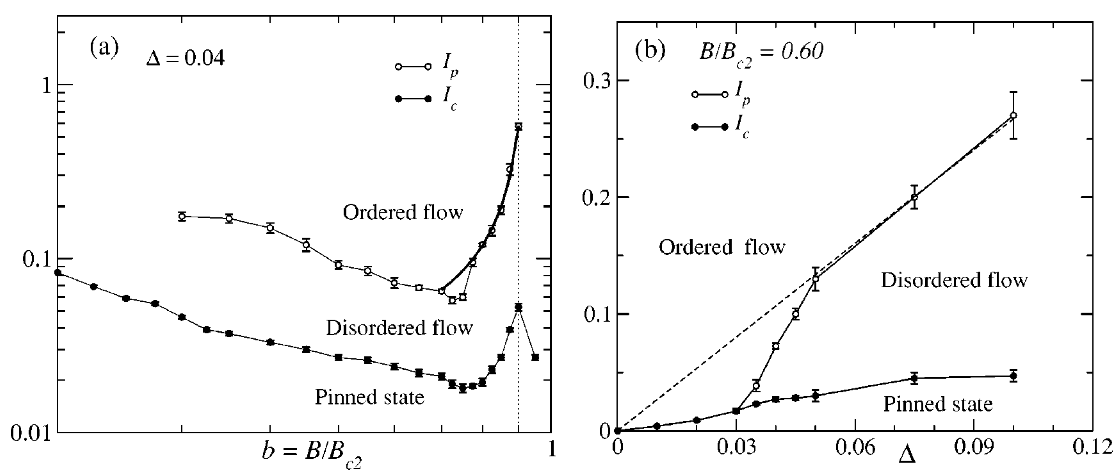

FIG. 4. (a) The dynamic phase diagram showing $I_p(b)$ and $I_c(b)$ for $\Delta = 0.04$. The thick line is a fit to $I_p(b) \sim (b_0 - b)^{-1}$ in the peak effect regime. (b) The I_p and I_c as a function of Δ for $b = 0.60$. The dashed line is a linear fit to the data in the range $\Delta \geqslant 0.05$.

weak to strong pinning occurs for Δ between 0.03 and 0.05, and is also the range in which a sharp dynamic transition is observed. We find that for the intermediate pinning the real space configuration at $I=0$ show domains of ordered lattice separated by domain walls. The presence of ordered region ensures that the distribution of $v_x \propto 1/T_{\mathrm{sh}}$ is narrow which consequently gives a sharp dynamic transition. On the other hand, increasing Δ above 0.05 decreases the domain size to $\sim 2-3a_0$. This leads to a broader distribution of v_x which in turn broadens the dynamic transition. Thus, a sharp dynamic transition at I_p implies the existence of ordered regions with a narrow distribution of the domain size. In Ref. 17, the coexistence of the ordered and the disordered regions was shown to underlie the shape of the $V(I)$ curves in the vicinity of the PE. The disordered state in Ref. 17 is thought to appear due to the injection of vortices across the surface barrier. Our simulation suggests that the shape of the $V(I)$ curve depends crucially on the distribution of the size of the ordered domains in equilibrium.

In conclusion, we have shown that for disordered type-II superconductors, the dynamic transition current I_p and the critical current I_c shows similar behavior as the magnetic field B is varied. I_p decreases with B for fields below the PE regime. In the peak effect regime, $I_p(B)$ increases rapidly along with the $I_c(B)$. The dynamic transition is sharp for the intermediate pinning strength due to the presence of large domains of ordered vortex lattice in equilibrium.

M.C. acknowledges useful discussions with E. Zeldov during the course of the work, and thanks the University of New Mexico for access to their Albuquerque High Performance Computing Center. This work was supported by Grant No. NSF-DMR 9985978.

*Electronic address: chandran@physics.ucdavis.edu

[1] An-Chang Shi and A.J. Berlinsky, Phys. Rev. Lett. **67**, 1926 (1991); H.J. Jensen, A. Brass, and A.J. Berlinsky, *ibid.* **60**, 1676 (1988).

[2] A.E. Koshelev and V.M. Vinokur, Phys. Rev. Lett. **73**, 3580 (1994).

[3] T. Giamarchi and P. Le Doussal, Phys. Rev. Lett. **76**, 3408 (1996).

[4] S. Scheidl and V.M. Vinokur, Phys. Rev. E **57**, 2574 (1998).

[5] L. Balents, M.C. Marchetti, and L. Radzihovsky, Phys. Rev. B **57**, 7705 (1998).

[6] K. Moon, R.T. Scalettar, and G.T. Zimányi, Phys. Rev. Lett. **77**, 2778 (1996).

[7] C.J. Olson, C. Reichhardt, and F. Nori, Phys. Rev. Lett. **81**, 3757 (1998).

[8] A.B. Kolton, D. Domínguez, and N. Grønbech-Jensen, Phys. Rev. Lett. **83**, 3061 (1999).

[9] H. Fangohr, S.J. Cox, and P.A.J. de Groot, Phys. Rev. B **64**, 064505 (2001).

[10] At still higher force, the smectic phase goes over to moving Bragg glass in 3D for weak disorder (Ref. 3).

[11] U. Yaron, P.L. Gammel, D.A. Huse, R.N. Kleimann, C.S. Oglesby, E. Bucher, B. Batlogg, D.J. Bishop, K. Mortensen, and K.N. Clausen, Nature (London) **376**, 753 (1995).

[12] S. Bhattacharya and M.J. Higgins, Phys. Rev. Lett. **70**, 2617 (1993); M.J. Higgins and S. Bhattacharya, Physica C **257**, 232 (1996).

[13] A. Duarte, E. Fernandez Righi, C.A. Bolle, F. de la Cruz, P.L. Gammel, C.S. Oglesby, E. Bucher, B. Batlogg, and D.J. Bishop, Phys. Rev. B **53**, 11 336 (1996); F. Pardo, F. de la Cruz, P.L. Gammel, E. Bucher, and D.J. Bishop, Nature (London) **396**, 348 (1998).

[14] Mahesh Chandran, R. T. Scalettar, and G. T. Zimányi (unpublished).

[15] Mahesh Chandran, cond-mat/0103263 (unpublished).

[16] Mahesh Chandran (unpublished).

[17] Y. Paltiel, Y. Myasoedov, E. Zeldov, G. Jung, M.L. Rappaport, D.E. Feldman, M.J. Higgins, and S. Bhattacharya, Phys. Rev. B **66**, 060503(R) (2002).